ChemEurJ

Research Article
doi.org/10.1002/chem.202502450

Chemistry Europe
European Chemical Societies Publishing

www.chemeurj.org

(2-Phosphinophenyl)aluminum Dichloride Complexes as Intramolecular Al/P Frustrated Lewis Pairs for Ketone, Ester, and Imine Activation

Yoshihiro Nishimoto,*[a, b, c] Hirotaka Okamoto,[a] and Makoto Yasuda*[a, b]

(2-Phosphinophenyl)aluminum dichloride complexes were synthesized and their frustrated Lewis pair (FLP) reactivity was investigated. Selective mono-substitution of $AlCl_3$ with lithioarenes was achieved by introducing sterically demanding substituents—*tert*-butyl, ethyl, or PCy_2—at the 6-position of the phenylene linker, effectively suppressing over-substitution and enabling successful isolation of the target complexes. Single-crystal X-ray diffraction and NMR spectroscopic analyses confirmed the formation of a four-membered P–Al–C–C core structure. These complexes function as Al/P-based FLPs capable of activating simple carbonyl and imine compounds, including aliphatic ketones, prop-2-ynoate esters, and *N*-arylimines. The mechanism of carbonyl activation by these Al/P FLPs was elucidated through density functional theory (DFT) calculations.

1. Introduction

Over the past decade, research related to frustrated Lewis pairs (FLPs) has grown substantially as these systems have the unique ability to activate small molecules and promote a plethora of catalytic transformations.[1–9] Intermolecular FLP systems require substantial steric hindrance for maintaining spatial separation between the Lewis acidic and basic centers. In contrast, intramolecular FLPs are constructed by covalently linking a Lewis acid and base through a bridging unit (linker).[10] A key advantage of intramolecular FLPs over their intermolecular counterparts is the ability to control the spatial arrangement and distance between the reactive centers by tuning the linker structure.[11] Despite the development of numerous intramolecular FLP systems based on boron-containing Lewis acids, reports on Al-based Lewis acids are relatively limited.[12] Aluminum is among the most earth-abundant elements and aluminum compounds are generally less toxic and more cost-effective than transition metal complexes; thus, the development of FLP systems incorporating aluminum-based Lewis acids is promising for the advancement of sustainable chemical processes. The HOMO–LUMO gap between the Lewis acid and base plays a central role in the FLP reactivity. In this context, the inherently high Lewis acidity of aluminum offers a notable advantage over boron-based systems.[13] To date, most intramolecular aluminum-based FLPs feature hydrocarbyl (alkyl or aryl) substituents at the aluminum center.[12] Such FLPs have been employed to activate carbonyl compounds and their analogs—including CO_2,[12] aldehydes,[12] isocyanates,[12] diketones,[14] α,β-unsaturated carbonyl compounds,[14] cyclopropenones,[14] benzonitrile,[15] and azirines.[16] However, the activation of simple ketones, esters, and imines remains underdeveloped (Figure 1A). Enhancing the Lewis acidity of aluminum centers by introducing highly electronegative halogen substituents is a promising strategy for

[a] Dr. Y. Nishimoto, H. Okamoto, Prof. Dr. M. Yasuda
Department of Applied Chemistry, Graduate School of Engineering, The University of Osaka, 2-1 Yamadaoka, Suita, Osaka 565–0871, Japan
E-mail: nishimoto@chem.eng.osaka-u.ac.jp
yasuda@chem.eng.osaka-u.ac.jp

[b] Dr. Y. Nishimoto, Prof. Dr. M. Yasuda
Innovative Catalysis Science Division, Institute for Open and Transdisciplinary Research Initiatives (ICS-OTRI), The University of Osaka, 2-1 Yamadaoka, Suita, Osaka 565–0871, Japan

[c] Dr. Y. Nishimoto
PRESTO, Japan Science and Technology Agency (JST), Kawaguchi, Saitama 332–0012, Japan

Supporting information for this article is available on the WWW under https://doi.org/10.1002/chem.202502450

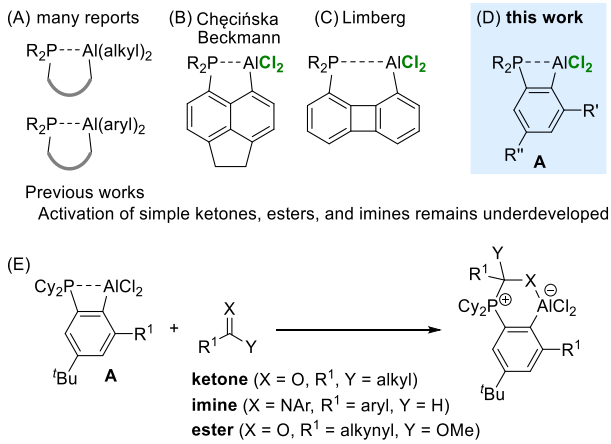

Figure 1. Reported intramolecular FLPs containing aluminium dihalide moiety as Lewis acid versus this work.

enabling the activation of these challenging substrates. Despite this potential, only two intramolecular FLPs bearing aluminum dihalide moieties have been reported to date.[17,18] Chęcińska and Beckmann reported the synthesis and structural characterization of [5-(diarylphosphino)acenaphth-6-yl]aluminum dichloride (Figure 1B),[19] although its FLP reactivity was not demonstrated owing to strong intramolecular Lewis acid–base interactions resulting from the short Al–P distance. Limberg et al. reported the reactivity of Al/P FLP based on a biphenylene structure, in which appropriate spatial separation between the Ar_2P and $AlCl_2$ moieties enabled activation of the CO_2 and allene (Figure 1C).[11] This study presents the synthesis, characterization, and FLP reactivity of (2-phosphinophenyl)aluminum dichloride complex **A** possessing substituents at the 4- and 6-positions (Figure 1D). Notably, these complexes effectively activate aliphatic ketone, *N*-arylimine, and prop-2-ynoate ester substrates (Figure 1E). To the best of our knowledge, this is the first report of the activation of carbonyl and iminyl groups in simple ketones, imines, and esters by FLP based on Al-Lewis acids.

2. Results and Discussion

In cases where the Lewis acidity of the aluminum center is significantly enhanced by the halogen atoms in the target **A** (Figure 1D), intramolecular coordination of the phosphorus atom may be excessively strengthened, thereby inhibiting the expression of FLP characteristics. The use of an *ortho*-phenylene bridge to tether the Lewis acidic and basic sites enables the manifestation of frustrated Lewis pair (FLP) reactivity, driven by the release of ring strain associated with the four-membered Al–P–C–C ring. Since the seminal work of Miqueu and Borissou on *ortho*-phenylene-bridged B/P-based FLPs (Figure 2A-i),[20] the design of vicinal FLP systems incorporating phenylene linkers has been established as an efficient strategy for developing intramolecular FLPs.[1–9] However, systems incorporating an aluminum dihalide moiety (AlX_2) remain unprecedented (Figure 2A-ii). Bourissou et al. reported the synthesis of $Al[C_6H_4(o\text{-}P^iPr_2)]_2Cl$ via the reaction of $AlCl_3$ with *ortho*-lithio $PPh(i\text{-}Pr)_2$ in a 1:2 molar ratio (Figure 2A-iii).[21,22] Similarly, Fontaine et al. prepared $Al[C_6H_4(o\text{-}PPh_2)]_3$ by reacting $AlCl_3$ with *ortho*-lithio PPh_3 in a 1:3 molar ratio (Figure 2A-iv).[23,24] Very recently, Breher et al. reported the synthesis and reactivity of $Al[C_6H_4(o\text{-}PPh_2)](^tBu)_2$ as an FLP; however, they did not address the activation of ketones, imines, or esters (Figure 2A-v).[25] In addition to *ortho*-phenylene-bridged FLPs, Mizuhata and Tokitoh reported the synthesis of vicinal C_2-bridged Al/P FLPs capable of activating benzaldehyde and alkynes. (Figure 2A-vi).[26,27] Initially, the synthesis of $Al[C_6H_4(o\text{-}PPh_2)]Cl_2$ was attempted herein; however, the reaction yielded a mixture of $Al[C_6H_4(o\text{-}PPh_2)_nCl_{3-n}]$ species (n = 1, 2, 3) via over substitution (Figure 2B), even under stoichiometric 1:1 reaction conditions (see the Supporting Information for details).[28] To address this issue, a substituent, *tert*-butyl, ethyl, or PCy_2, was introduced at the 6-position of the phenylene linker to suppress multiple substitutions (Figure 2C).[31,32]

The lithiation of aryl bromide precursors **B-1** and **B-2** with ^{n}BuLi, followed by a substitution reaction between $AlCl_3$ and the corresponding lithioarenes successfully afforded the target Al/P FLPs **A-1** and **A-2** (Scheme 1A), respectively. A *tert*-butyl group was introduced to facilitate the synthesis and improve solubility. These complexes were isolated as air- and moisture-sensitive solids through evaporation of the volatiles, followed by filtration and washing with heptane and pentane. The signals of **A-1** and **A-2** in the $^{27}Al\{^1H\}$ NMR spectra in CD_2Cl_2 at δ = 117.5 and

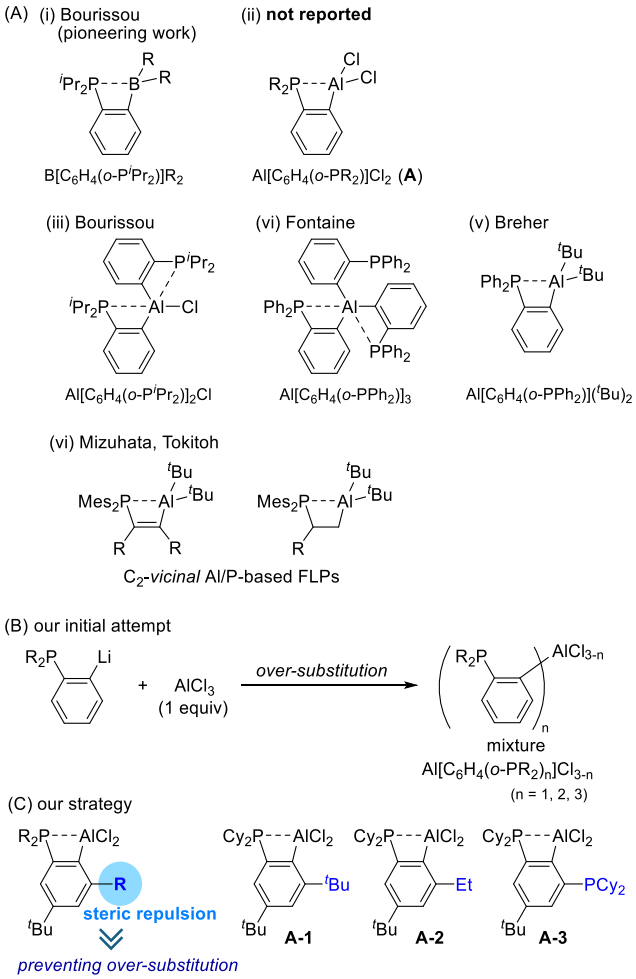

Figure 2. A) *ortho*-Phenylene-bridged Al/P-based FLPs. B) Initial attempt to synthesize $Al[(o\text{-}Ph_2P)C_6H_4]Cl_2$. C) Developed strategy for suppressing multiple substitution.

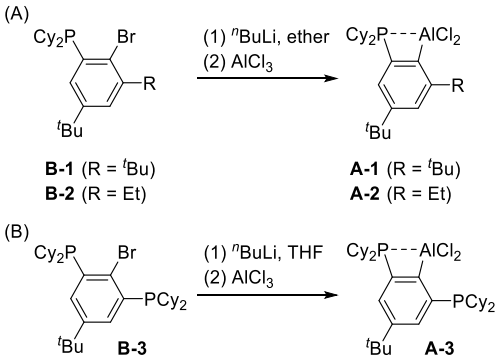

Scheme 1. Syntheses of **A-1**, **A-2**, and **A-3** via reaction of $AlCl_3$ with lithioarenes.

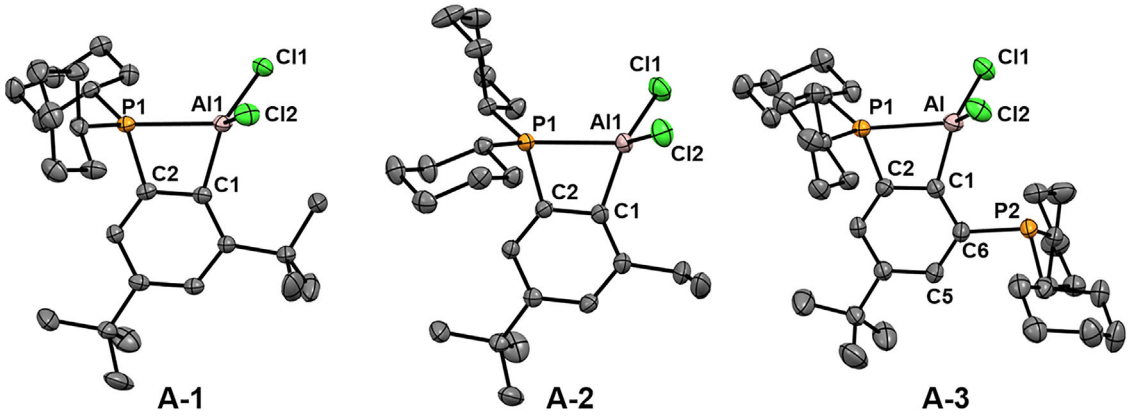

Figure 3. Molecular structures of **A-1**, **A-2**, and **A-3** showing 30% probability ellipsoids. Hydrogen atoms are omitted for clarity. Selected bond lengths (Å) and angles (°): **A-1**: Al1–P1 = 2.444(1), Al1–C1 = 1.978(3), P1–C2 = 1.824(3), P1–C2–C1 = 108.5(2), Al1–C1–C2 = 103.0(2), Cl1–Al1–Cl2 = 110.20(5), Cl1–Al1–C2 = 121.5(1), C1–Al1–Cl2 = 119.6(1), P1–Al1–C1 = 72.33(9). **A-2**: Al1–P1 = 2.4632(6), Al1–C1 = 1.963(2), P1–C2 = 1.813(2), P1–C2–C1 = 108.5(1), Al1–C1–C2 = 103.8(1), Cl1–Al1–Cl2 = 108.96(3), Cl1–Al1–C2 = 119.25(6), C1–Al1–Cl2 = 121.15(6), P1–Al1–C1 = 71.76(5). **A-3**: Al–P1 = 2.494(2), Al–P2 = 3.585(2), Al–C1 = 1.964(5), P1–C2 = 1.825(5), P1–C2–C1 = 107.7(4), Al–C1–C2 = 105.8(4), Al–C1–C6 = 136.3(4), Cl1–Al–Cl2 = 110.50(9), Cl1–Al–C2 = 118.2(2), C1–Al–Cl2 = 124.3(2), C1–C6–P2 = 114.2(4), C5–C6–P2 = 126.4(4), P1–Al1–C1 = 70.6(2).

117.7 ppm, respectively, are similar to the reported chemical shifts of tetra-coordinate aluminum atoms in $ArAlCl_2$ with an internal coordinating group.[31–33] Signals of **A-1** and **A-2** were observed at δ = 29.5 and 33.7 ppm, respectively, in the $^{31}P\{^1H\}$ NMR spectra, where the signals were significantly shifted downfield relative to that of free PCy_2Ph (δ = 6.3 ppm). Single-crystal X-ray diffraction (SC-XRD) analyses[34] of **A-1** and **A-2** confirmed the installation of an $AlCl_2$ moiety adjacent to the PCy_2 unit at the 1,2-positions on the phenylene scaffold (Figure 3). In the respective complexes, the P–Al bond length is 2.444(1) Å and 2.4632(6) Å and the ratio (*r*) between these distances and the sum of the covalent radii (2.28 Å)[35] is *r* = 1.07 and 1.08, suggesting effective coordination of phosphorus to the aluminum atoms. The $AlCl_2$ and PCy_2 substituents were inclined toward each other. The bay angles (P1–C2–C1 = 108.5(2)°, Al1–C1–C6 = 103.0(2)° for **A-1**, P1–C2–C1 = 108.5(1)°, and Al1–C1–C6 = 103.9(1)° for **A-2**) deviated substantially from the ideal value of 120°, reflecting the significant ring strain associated with the Al–P–C–C four-membered ring. The tetrahedral character (THC) values for **A-1** (24%) and **A-2** (22%) indicate highly distorted tetrahedral geometries at the Al centers, together with acute P1–Al–C1 angles (72.33(9)° and 71.76(5)°, respectively).[36] Following the same synthetic strategy, complex **A-3** was synthesized from aryl bromide precursor **B-3** bearing two PCy_2 substituents (Scheme 1B). SC-XRD analysis revealed that one of the two PCy_2 groups is inclined toward the $AlCl_2$ moiety, with a short Al1–P1 distance of 2.494(2) Å, indicating a donor–acceptor interaction. In contrast, the Al1–P2 distance is much longer (3.585(2) Å), suggesting a weak interaction. **A-3** also exhibits a highly distorted tetrahedral geometry, as evidenced by its low THC value (21%) and acute P1–Al–C1 angle (70.6(2)°). The $^{27}Al\{^1H\}$ NMR spectrum in CD_2Cl_2 shows a resonance at δ = 118.7 ppm, consistent with tetra-coordinate aluminum. Contrary to expectations based on the solid-state structure, the $^{31}P\{^1H\}$ NMR spectrum of **A-3** in CD_2Cl_2 at room temperature exhibits a single, sharp signal at δ = 23.0 ppm. This chemical shift is between those of **A-1** and $PhPCy_2$. This peak was not split but showed slight broadening at −50 °C (Figure S4), suggesting a

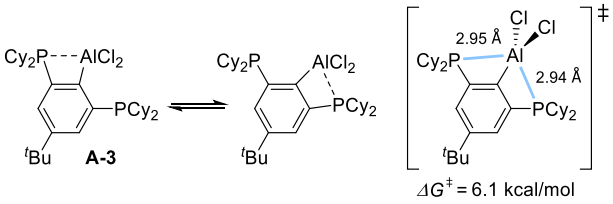

Scheme 2. Equilibrium for the coordination of two P atoms to the Al atom in **A-3**. DFT calculations were carried out with the SMD(CH_2Cl_2)-ωB97XD /6–311G(d,p)//SMD(CH_2Cl_2)-ωB97XD/6–31G(d) functional.

fast equilibrium between coordination and noncoordination of the two phosphorus atoms to the aluminum center in solution, as depicted in Scheme 2. Density functional theory (DFT) calculations support this interpretation, indicating a low activation barrier ($\Delta G^{\ddagger}$ = 6.1 kcal/mol) for the interconversion. In the transition state, the Al–P distances are equivalent, and the sum of the bond angles around the aluminum atom (Cl–Al–Cl = 110.957°, Cl–Al–C = 124.497° or = 124.546°) is 360°, which is consistent with the trigonal planar geometry.

The Lewis acidity of complexes **A** was evaluated based on the $\Delta\nu$(C = O) values of pyrone **1** upon complexation with **A** (Scheme 3).[37] The $\Delta\nu$(C = O) values of complexes **A-1**, **A-2**, and **A-3**[34] are comparable to that of $AlCl_3$, indicating their potentially high Lewis acidity. The molecular structures of the resulting complexes **A•1** are shown in Figure S5. In all cases, the carbonyl oxygen atom of **1** displaced the intramolecular phosphorus atom and coordinated with the Al atom. The THC values of the **A•1** complexes—44% for **A-1•1**, 65% for **A-2•1**, and 64% for **A-3•1**—are significantly higher than those of the corresponding uncoordinated complexes **A**. The strain release of the four-membered ring drives the dissociation of the intramolecular Cy_2P group from the aluminum atom. These results demonstrate that complex **A** exhibits pronounced Lewis acidity toward external Lewis bases.

Considering the high Lewis acidity of complex **A**, its ability to activate carbonyl compounds was investigated. The reactions of **A-1** and **A-2** with heptan-4-one (**2**) in CD_2Cl_2 at room temperature

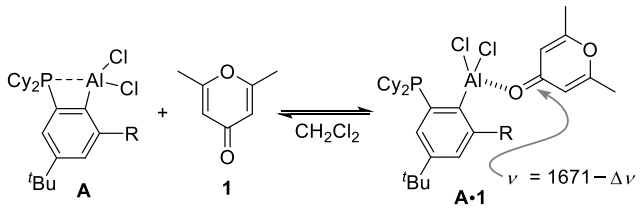

Al compound	$\Delta\nu$ (cm^{-1})
A-1	17
A-2	18
A-3	17
$AlCl_3$	20

Scheme 3. Evaluation of Lewis acidity of **A** based on $\Delta\nu$(C = O) value of pyrone **1**.

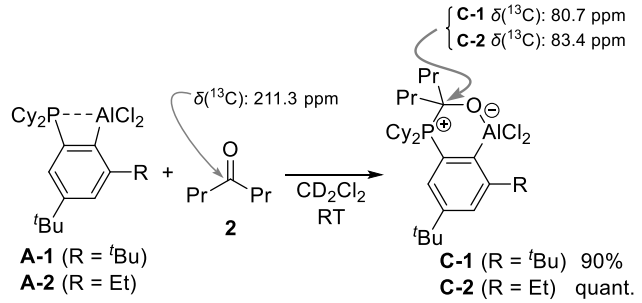

Scheme 4. Activation of ketone **2** by **A-1** and **A-2**.

afforded the corresponding ketone adducts **C-1** and **C-2** in excellent yields (Scheme 4). In the $^{13}C\{^1H\}$ NMR spectra, the resonance corresponding to the carbonyl carbon of **2** disappeared, and characteristic doublets appeared at δ = 80.7 and 83.4 ppm with $^1J_{C,P}$ coupling constants of 40.2 and 35.9 Hz, respectively. These signals correspond to the carbon atoms originating from the carbonyl group of **2**, which are bound to the phosphorus atoms in **C-1** and **C-2**. The observed ^{13}C chemical shifts are comparable to that of the reported α-alkoxy-substituted phosphonium compound, $Ph_3P^+C(CH_3)_2OCH_2C(CH_3)_2O^-$ (δ = 75.5 ppm).[38,39] The $^{31}P\{^1H\}$ NMR spectra of **C-1** and **C-2** display resonances at δ = 31.7 and 24.8 ppm, respectively. These values are close to those previously reported for phosphonium species (e.g., $^{31}P\{^1H\}$ NMR: $Ph_3P^+C(CH_3)_2OCH_2C(CH_3)_2O^-$; δ = 30.5 ppm, $Bu_3(Ph)P^+Cl^-$; δ = 30.1 ppm).[38,39] The ^{27}Al NMR signals of **C-1** and **C-2** appeared upfield relative to those of **A-1** and **A-2** (**C-1**: δ = 96.0 ppm, **C-2**: δ = 98.5 ppm). Although suitable single crystals of **C-1** were not obtained, the molecular structure of **C-2** was successfully determined using SC-XRD analysis (Figure 4).[34] When the phosphorous substituent at aluminium atom was replaced with an oxygen atom, the strain in the four-membered ring was relieved, and the aluminum center in **C-2** adopted a more tetrahedral geometry (higher tetrahedral character) than that in **A-2**. The P1–C3 distance of 1.905(4) Å and ratio (*r*) relative to the sum of the covalent radii (1.83 Å) of 1.04 support the formation of a P–C bond. The high THC of 88% indicates that the C3 atom was sp^3-hybridized. The bonds formed between Al and the carbonyl O atoms and between P and the carbonyl C atoms constructed an Al—C—C—P—C—O six-membered ring. As anticipated, the aluminum and phosphorus atoms functioned as Lewis acids and nucleophiles, respectively, cooperatively activating the carbonyl groups of **2**.

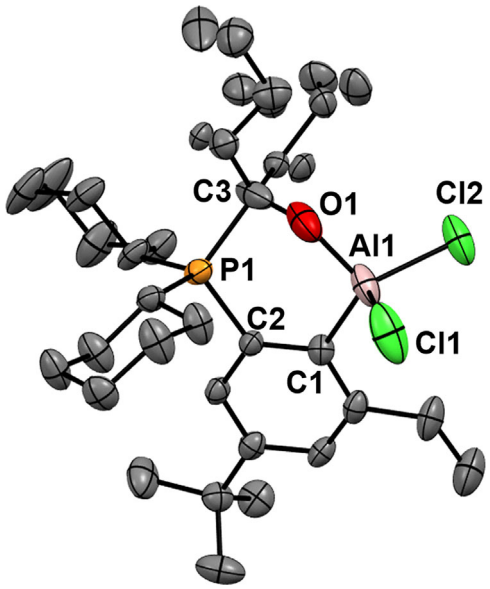

Figure 4. Molecular structure of **C-2** showing 30% probability ellipsoids. Hydrogen atoms and solvent molecule (CH_2Cl_2) are omitted for clarity. Two propyl groups are disordered. Selected bond lengths (Å) and angles (°): P1–C2 = 1.827(4), Al1–C1 = 1.987(4), Al1–O1 = 1.737(5), C3–O1 = 1.409(8), C3–P1 = 1.905(4), P1–C2–C1 = 122.6(2), Al1–C1–C2 = 121.0(3), Cl1–Al–Cl2 = 108.78(8), Cl1–Al–C1 = 112.7(1), C1–Al–Cl2 = 112.5(1), C1–Al–O1 = 104.9(2), O1–Al1–Cl1 = 107.0(1), O1–Al1–C2 = 110.8(1).

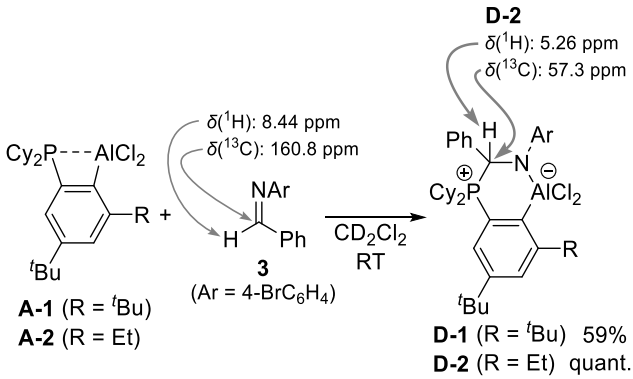

Scheme 5. Activation of imine **3** by **A-1** and **A-2**.

The treatment of imine **3** with **A-1** and **A-2** at room temperature afforded the corresponding adducts **D-1** and **D-2** (Scheme 5). **D-1** was obtained in moderate yield (59%) and was not isolated from the reaction mixture. In contrast, **D-2** was obtained quantitatively. The ^1H and $^{13}C\{^1H\}$ NMR spectra of **D-2** show resonances of the hydrogen and carbon atoms originating from the iminyl group at δ = 5.26 ppm and δ = 57.3 ppm, respectively. The $^2J_{H,P}$ coupling constant was 18.9 Hz and the $^1J_{C,P}$ coupling constant was 51.8 Hz, indicating the formation of a P–C bond between the phosphorus atom and iminyl carbon. The ^{27}Al and ^{31}P NMR signals appeared at δ = 105.6 ppm and δ = 31.0 ppm, respectively, consistent with the trend observed for **C-1** and **C-2**. The solid-state molecular structure of **D-2** is shown in Figure 5.[34] As

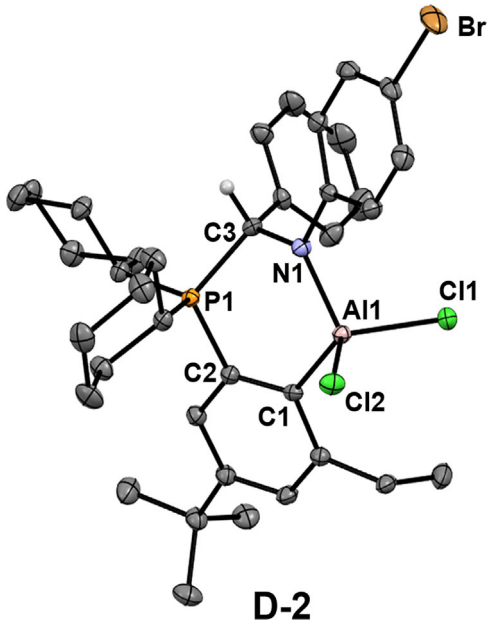

Figure 5. Molecular structure of **D-2** showing 30% probability ellipsoids. Hydrogen atoms are omitted for clarity, except hydrogen on C3. Selected bond lengths (Å) and angles (°): C2–P1 = 1.810(4), Al–N = 1.860(3), Al–C1 = 1.988(3), N1–C3 = 1.463(4), C3–P1 = 1.851(3), P1–C2–C1 = 116.5(3), Al–C1–C2 = 123.6(3), Cl1–Al–Cl2 = 108.81(5), Cl1–Al–C1 = 115.0(1), C1–Al–Cl2 = 107.8(1), C1–Al–N = 107.6(1).

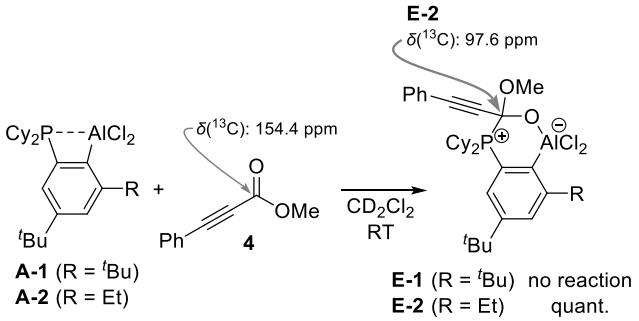

Scheme 6. Activation of ester **4** by **A-1** and **A-2**.

expected, the formation of both Al1–N1 and P1–C3 bonds was confirmed. The aluminum atom adopted a tetrahedral geometry, forming a six-membered Al–C–C–P–C–N ring (THC for Al1:86%). The P1–C3 bond length was 1.851(3) Å. The geometry of the C3 atom changed from trigonal planar in imine **3** to tetrahedral in **D-2**, as evidenced by the THC (74%) of the former. The C3–N1 bond length was 1.463(4) Å, consistent with single-bond character of the C–N bond.

The activation of esters is more challenging than that of ketones and imines primarily because of the generally lower electrophilicity of the carbonyl groups in esters. Accordingly, the treatment of simple alkanoic esters such as ethyl acetate with **A-1** and **A-2** did not result in any reaction. Gratifyingly, the reaction of methyl 3-phenyl-prop-2-ynoate (**4**) with **A-2** at room temperature proceeded smoothly to afford the adduct **E-2**, likely because of the reduced steric hindrance associated with the alkynyl moiety (Scheme 6). In contrast, no reaction was observed between **A-1** and **4**. **E-2** was characterized through a series of NMR spectroscopic analyses. The ^{27}Al and ^{31}P NMR signals appeared at δ = 99.9 ppm and δ = 25.4 ppm, respectively. These values are close to those observed for **C-2** and **D-2**. The resonance at δ = 97.6 ppm with a $^{1}J_{C,P}$ coupling constant of 96.8 Hz in the $^{13}C\{^{1}H\}$ NMR spectrum corresponds to the carbon atom originating from the carbonyl carbon of **4**, indicating the formation of a P–C bond. The molecular structure of **E-2** was confirmed using SC-XRD, which revealed a six-membered Al–C–C–P–C–O ring (Figure 6).[34] The aluminum atom is coordinated to the carbonyl oxygen atom (Al1–O1 = 1.761(3) Å) and adopts a tetrahedral geometry (THC = 80%). The P1–C3 bond is clearly observed, with a bond length of 1.889(5) Å. Mizuhata and Tokitoh reported that a vicinal C_2-bridged Al/P FLP (Figure 2A-vi, left) reacts with dimethyl acetylenedicarboxylate (DMAD) by 1,3- rather than 1,2-addition and, moreover, does not activate **4**.[26] This contrasts markedly with the present complex **A-2**, which activates **4** via a 1,2-addition.[40]

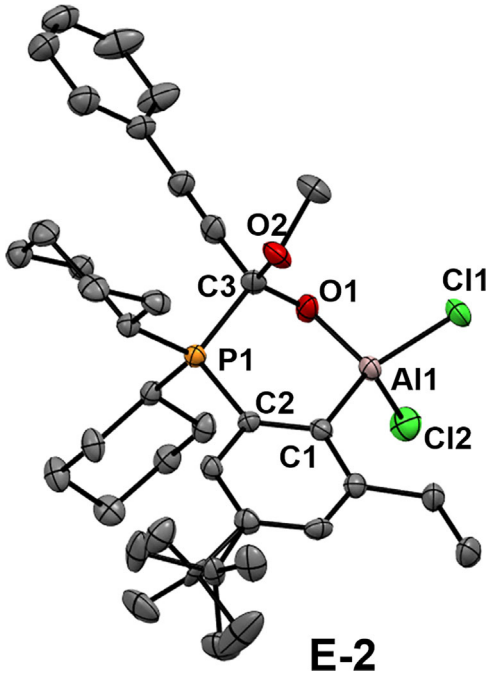

Figure 6. Molecular structure of **E-2** showing 30% probability ellipsoids. Hydrogen atoms and solvent molecule (CH_2Cl_2) are omitted for clarity. ^{t}Bu group is disordered. Selected bond lengths (Å) and angles (°): P1–C2 = 1.803(4), Al1–C1 = 1.972(4), Al1–O1 = 1.761(3), C3–O1 = 1.376(5), C3–P1 = 1.889(5), P1–C2–C1 = 116.5(3), Al–C1–C2 = 123.6(3), Cl1–Al–Cl2 = 107.67(7), Cl1–Al–C1 = 112.8(1), C1–Al–Cl2 = 114.4(1), C1–Al–O1 = 106.6(2), O1–Al1–Cl1 = 110.0(1), O1–Al1–C2 = 104.9(1).

Subsequently, the reactivity of **A-3** toward ketone **2**, imine **3**, and ester **4** was examined. All three reactions proceeded smoothly at room temperature to quantitatively afford the corresponding adducts **C-3**, **D-3**, and **E-3**, respectively (Scheme 7). The structures of these products were unambiguously confirmed using SC-XRD (Figure 7).[34] In the solid state, one (P1) of the two phosphorus atoms in each complex forms a bond with the carbonyl or iminyl carbon atom, resulting in the formation of a P1–C3 bond. Simultaneously, the carbonyl oxygen or iminyl nitrogen atom coordinates to the aluminum center, affording six-membered rings of the type Al–C–C–P–C–O (for **C-3** and **E-3**)

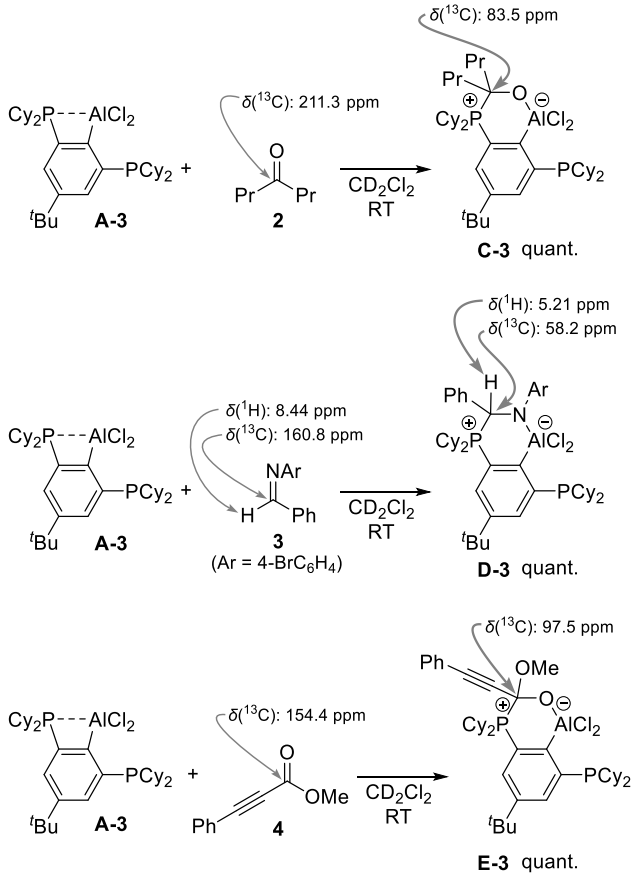

Scheme 7. Activation of ketone **2**, imine **3**, and ester **4** by **A-3**.

or Al–C–C–P–C–N (for **D-3**). The aluminum centers adopt tetrahedral geometries in all cases, as indicated by the THC values of 69% (**C-3**), 71% (**D-3**), and 70% (**E-3**). The second phosphorus atom did not participate in activation of the carbonyl or iminyl groups. The Al1–P2 distances in **C-3** (3.3483(7) Å), **D-3** (3.4260(9) Å), and **E-3** (3.292(3) Å) are significantly longer than the sum of the covalent radii (2.28 Å), supporting the absence of interaction. The $^{31}P\{^{1}H\}$ NMR spectra of **C-3**, **D-3**, and **E-3** show two distinct resonances for each complex: **C-3**: $\delta = 24.3$ and 4.7 ppm, **D-3**: $\delta = 30.9$ and 2.3 ppm, **E-3**: $\delta = 23.8$ and 5.8 ppm. The downfield signals correspond to the phosphorus atoms involved in carbonyl or iminyl activation and are comparable to the chemical shifts observed for **C-2**, **D-2**, and **E-2**. The chemical shift values of the more upfield resonances are close to that of Cy_2PhP ($^{31}P\{^{1}H\}$ NMR: $\delta = 6.3$ ppm). The $^{13}C\{^{1}H\}$ NMR spectra show signals of the carbon atoms originating from the carbonyl groups in **C-3** and **E-3**, and of the iminyl group in **D-3**, at $\delta = 83.5$, 97.5, and 58.2 ppm with $^{1}J_{C,P}$ coupling constants of 35.6, 96.0, and 52.6 Hz, respectively. The ^{1}H NMR spectrum of **D-3** shows a signal of the hydrogen atom originating from the iminyl group at $\delta = 5.21$ ppm, with a $^{2}J_{H,P}$ coupling constant of 18.5 Hz. The ^{27}Al NMR spectra of **C-3**, **D-3**, and **E-3** exhibit resonances around 100 ppm (**C-3**: $\delta = 93.6$ ppm; **D-3**: $\delta = 101.3$ ppm; **E-3**: $\delta = 94.1$ ppm), indicating the tetra-coordinated geometry of the aluminum atoms. Therefore, these results indicate that the molecular structures of **C-3**, **D-3**, and **E-3** in the solid state were maintained in solution.

Notably, **A-2** and **A-3** were more effective for activating the carbonyl and iminyl groups than **A-1**, as shown in Schemes 4–7.[41] To gain mechanistic insights into this reactivity trend, the reactions of **A-1**, **A-2**, and **A-3** with ester **4** were evaluated through DFT calculations. The computed reaction energy profiles are shown in Figure 8. In the reactions of **A-1** and **A-2** with **4**, the initial coordination of the carbonyl oxygen atom to the aluminum center leads to dissociation of the Al–P interaction, forming intermediates **Int1** and **Int2**. Subsequently, intramolecular nucleophilic attack by the phosphorus atom on the carbonyl group generates the corresponding adducts **E-1** and **E-2**. The reaction with **A-1** is endergonic

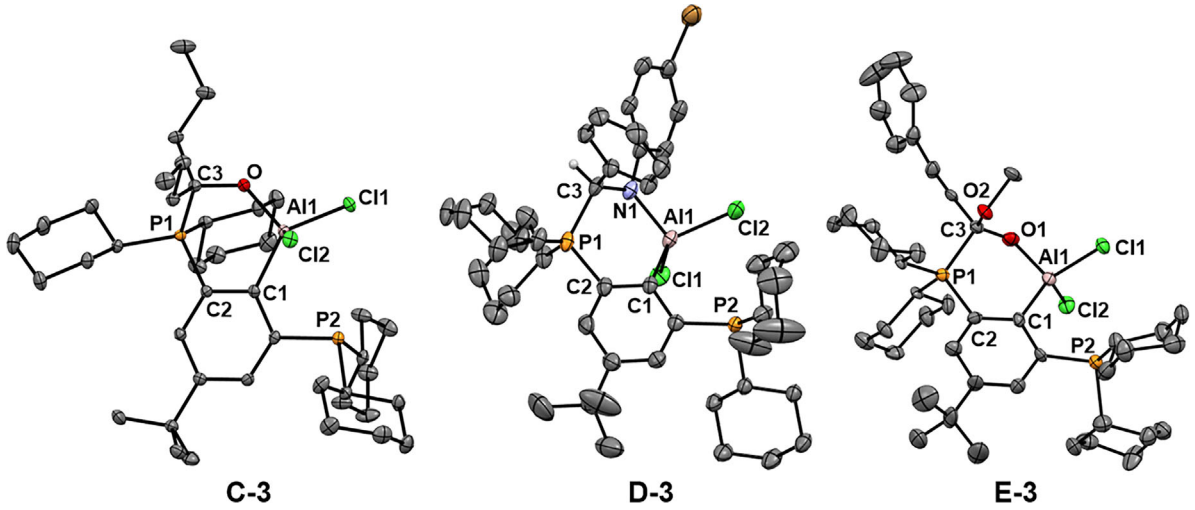

Figure 7. Molecular structures of **C-3**, **D-3**, and **E-3** showing 30% probability ellipsoids. Hydrogen atoms and solvent molecules are omitted for clarity. For **D-3**, a hydrogen atom on C3 is shown. Selected bond lengths (Å) and angles (°): **C-3**: C3–P1 = 1.894(2), Al1–O1 = 1.747(1), Al1–P2 = 3.3483(7), O1–C3 = 1.397(2), P1–C2–C1 = 119.3(1), Al1–C1–C2 = 120.7(1), Cl1–Al1–Cl2 = 108.96(3), Cl1–Al–C1 = 121.42(5), C1–Al–Cl2 = 107.41(5). **D-3**: C3–P1 = 1.845(2), Al1–N2 = 1.878(2), Al1–P2 = 3.4260(9), C3–N1 = 1.467(3), P1–C2–C1 = 120.5(2), Al1–C1–C2 = 120.2(2), Cl1–Al1–Cl2 = 109.50(4), Cl1–Al1–C1 = 102.00(7), C1–Al1–Cl2 = 122.61(8). **E-3**: C3–P1 = 1.887(7), Al1–O1 = 1.762(5), Al1–P2 = 3.292(3), C3–O1 = 1.342(9), P1–C2–C1 = 120.6(6), Al1–C1–C2 = 125.0(6), Cl1–Al–Cl2 = 108.7(1), Cl1–Al–C2 = 113.6(3), C1–Al–Cl2 = 117.8(3).

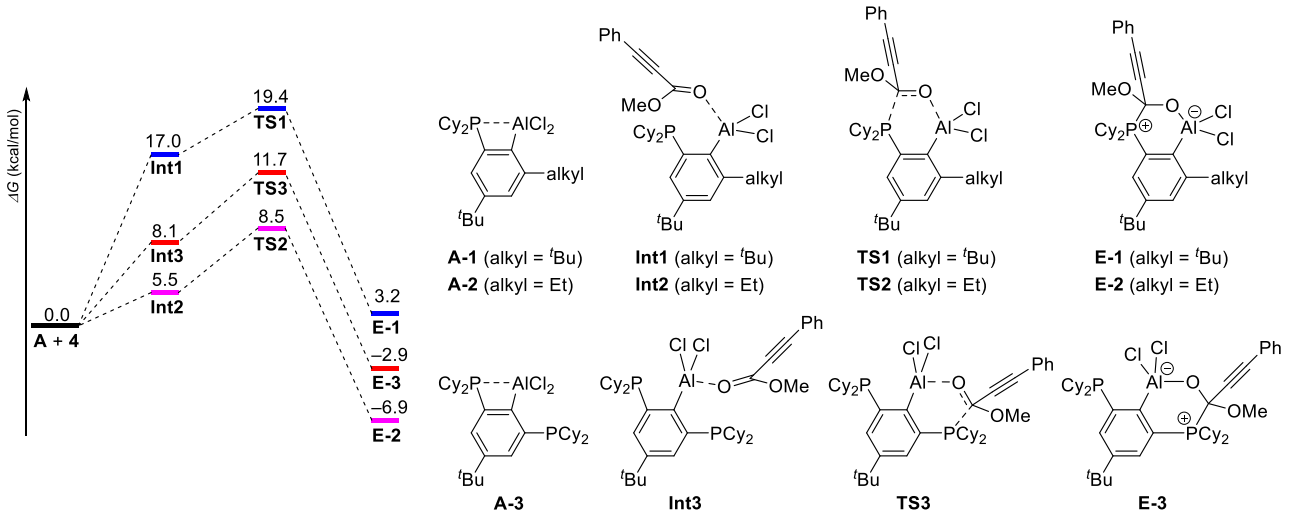

Figure 8. Computed profile for the addition reaction of **A** with **4**. DFT calculation was carried out with the SMD(CH_2Cl_2)-ωB97XD/6–311G(d,p)//SMD(CH_2Cl_2)-ωB97XD/6–31G(d) functional. The vertical axis represents relative Gibbs free energies (ΔG, kcal/mol at 298 K).

(ΔG = 3.2 kcal/mol), and the activation barrier is significantly higher ($\Delta G^{\ddagger}$ = 19.4 kcal/mol), which agrees with the experimental observation that **E-1** is not formed (Scheme 6). In contrast, the transformation of **A-2** is exergonic (ΔG = −6.9 kcal/mol) with an activation barrier of 8.5 kcal/mol, consistent with the effective production of **E-2** at room temperature (Scheme 6). Although the carbonyl group of **4** coordinates to the Al atom of **A-1**, the $AlCl_2$ moiety approaches the ^{t}Bu group, and the increased steric repulsion between the groups suppresses the addition reaction. A different activation pathway was identified for **A-3**. The carbonyl oxygen atom of **4** coordinates with the aluminum atom from the opposite side of the PCy_2 group, displacing this phosphorus atom. Subsequently, the PCy_2 group, positioned proximal to the carbonyl group via the phenylene linker, adds to the carbonyl group (**TS3**), leading to the formation of **E-3**. From the energy profile for the reaction of **A-3** with **4**, the activation barrier is 11.7 kcal/mol with a Gibbs free energy change of − 2.9 kcal/mol, in good agreement with the experimental formation of **E-3** at room temperature. A key feature common to both **A-1** and **A-3** is the effective activation of the carbonyl group by the $AlCl_2$ moiety, which facilitates nucleophilic attack by the PCy_2 group. In this process, the external Lewis basic substrate displaces an intramolecularly coordinating PCy_2 group from the aluminum center, thereby enhancing the Lewis acidity of the $AlCl_2$ moiety to a level sufficient for activation of ester **4**. The driving force for this transformation is the release of the ring strain associated with the four-membered Al–P–C–C structure. Additionally, the strategic positioning of the PCy_2 group adjacent to the $AlCl_2$ moiety via the phenylene linker is essential for promoting nucleophilic attack.

3. Conclusion

In summary, three (2-phosphinophenyl)aluminum dichloride complexes, **A-1**, **A-2**, and **A-3**, were synthesized, and their FLP properties were elucidated. The introduction of *tert*-butyl, ethyl, and PCy_2 substituents at the 6-position of the phenylene linker effectively suppressed multiple substitution reactions between $AlCl_3$ and lithioarenes, enabling successful isolation of the target complexes. Single-crystal X-ray diffraction and NMR spectroscopic analyses revealed that these aluminum complexes adopted four-membered P–Al–C–C ring structures. Complexes **A** activate aliphatic ketone **2**, *N*-arylimine **3**, and prop-2-ynoate ester **4**. DFT calculations of the reaction of **A** with ester **4** provided mechanistic insights into the activation of the carbonyl. The high Lewis acidity of the $AlCl_2$ unit and favorable spatial arrangement of the $AlCl_2$ and PCy_2 groups via the phenylene linker enable efficient activation of carbonyl and imine substrates. These findings highlight the potential of (2-phosphinophenyl)aluminum dichloride complexes as effective main-group FLP systems for small-molecule activation.

Supporting Information

Details of the instruments and methods, synthetic procedures, characterization data, and DFT calculations are provided in the Supporting Information.

The authors have cited additional references within the Supporting Information.[42–46]

Acknowledgments

This work was financially supported by JSPS KAKENHI grants (JP25K22182 (M.Y.), JP23K17845 (M.Y.) and JP24K22362 (Y.N.), a Grant-in-Aid for Transformative Research Areas (A) (JP21H05212 (M.Y.)) for Digitalization-driven Transformative Organic Synthesis (Digi-TOS) from the Ministry of Education, Culture, Sports, Science & Technology, Japan (MEXT), as well as by a JST CREST grant (JPMJCR20R3 (M.Y.)) and JST, PRESTO grant (JPMJPR24M7 (Y.N.)).

Conflict of Interest

The authors declare no conflict of interest.

Data Availability Statement

The data that support the findings of this study are available in the supplementary material of this article.

Keywords: aluminum · carbonyl activation · frustrated lewis pair · imine activation · phosphorus

[1] A selected review: D. W. Stephan, G. Erker, *Angew. Chem. Int. Ed.* **2010**, *49*, 46.
[2] A selected review: D. W. Stephan, G. Erker, *Chem. Sci.* **2014**, *5*, 2625.
[3] A selected review: D. W. Stephan, *Acc. Chem. Res.* **2015**, *48*, 306.
[4] A selected review: D. W. Stephan, *J. Am. Chem. Soc.* **2015**, *137*, 10018.
[5] A selected review: D. W. Stephan, G. Erker, *Angew. Chem. Int. Ed.* **2015**, *54*, 6400.
[6] A selected review: F.-G. Fontaine, M.-A. Courtemanche, M.-A. Légaré, É. Rochette, *Coord. Chem. Rev.* **2017**, *334*, 124.
[7] A selected review: J. Lam, K. M. Szkop, E. Mosaferi, D. W. Stephan, *Chem. Soc. Rev.* **2019**, *48*, 3592.
[8] A selected review: D. W. Stephan, *J. Am. Chem. Soc.* **2021**, *143*, 20002.
[9] A selected review: B. L. Frenette, E. Rivard, *Chem. Eur. J.* **2023**, *29*, e202302332.
[10] F.-G. Fontaine, D. W. Stephan, *Phil. Trans. R. Soc. A* **2017**, *375*, 20170004.
[11] P. Federmann, T. Bosse, S. Wolff, B. Cula, C. Herwig, C. Limberg, *Chem. Commun.* **2022**, *58*, 13451.
[12] A review of Al-based frustrated Lewis pairs: F. Krämer, *Angew. Chem. Int. Ed.* **2024**, *63*, e202405207.
[13] T. Kaehler, R. L. Melen, *Cell Rep. Phys. Sci.* **2021**, *2*, 100595.
[14] M. Lange, J. C. Tendyck, P. Wegener, A. Hepp, E.-U. Würthwein, W. Uhl, *Chem. Eur. J.* **2018**, *24*, 12856.
[15] L. Keweloh, H. Klçcker, E.-U. Würthwein, W. Uhl, *Angew. Chem. Int. Ed.* **2016**, *55*, 3212.
[16] D. Pleschka, M. Uebing, M. Lange, A. Hepp, A.-L. Wübker, M. R. Hansen, E.-U. Würthwein, W. Uhl, *Chem. Eur. J.* **2019**, *25*, 9315.
[17] Report of an intermolecular FLP system using a combination of aluminum trihalides with triarylphosphines: G. Ménard, D. W. Stephan, *Angew. Chem. Int. Ed.* **2011**, *50*, 8396.
[18] Report of an intermolecular FLP system using a combination of aluminum trihalides and triarylphosphines: G. Ménard, D. W. Stephan, *J. Am. Chem. Soc.* **2010**, *132*, 1796.
[19] E. Hupf, E. Lork, S. Mebs, L. Chęcińska, J. Beckmann, *Organometallics* **2014**, *33*, 7247–7259.
[20] S. Bontemps, G. Bouhadir, K. Miqueu, D. Bourissou, *J. Am. Chem. Soc.* **2006**, *128*, 12056.
[21] M. Sircoglou, G. Bouhadir, N. Saffon, K. Miqueu, D. Bourissou, *Organometallics* **2008**, *27*, 1675.
[22] M. Sircoglou, N. Saffon, K. Miqueu, G. Bouhadir, D. Bourissou, *Organometallics* **2013**, *32*, 6780–6784.
[23] M.-A. Courtemanche, J. Larouche, M.-A. Légaré, W. Bi, L. Maron, F.-G. Fontaine, *Organometallics* **2013**, *32*, 6804–6811.
[24] It is mentioned in ref. [19]that the selective synthesis of ArAlCl2 requires careful selection of the reaction conditions to avoid the generation of Ar2AlCl and Ar3Al via multiple substitutions.
[25] M. E. A. Dilanes, F. Breher, *Eur. J. Inorg. Chem.* **2025**, e202500174.
[26] T. Yanagisawa, Y. Mizuhata, N. Tokitoh, *ChemPlusChem* **2020**, *85*, 933.
[27] T. Yanagisawa, Y. Mizuhata, N. Tokitoh, *Chem. Eur. J.* **2021**, *27*, 11273.
[28] See details in the Supporting Information.
[29] R. J. Wehmschulte, P. P. Power, *Inorg. Chem.* **1996**, *35*, 3262.
[30] R. J. Wehmschulte, W. J. Grigsby, B. Schiemenz, R. A. Bartlett, P. P. Power, *Inorg. Chem.* **1996**, *35*, 6694.
[31] J. Muller, U. Englert, *Chem. Ber.* **1995**, *128*, 493.
[32] Y. Nishimoto, S. Nakao, S. Machinaka, F. Hidaka, M. Yasuda, *Chem. Eur. J.* **2019**, *25*, 10792.
[33] C. L. Lund, J. A. Schachner, I. J. Burgess, J. W. Quail, G. Schatte, J. Müller, *Inorg. Chem.* **2008**, *47*, 5992.
[34] Deposition Numbers 2470419 (for **A-1**), 2470361 (for **A-2**), 2470362 (for **A-3**), 2470427 (for **A-1•1**), 2470425 (for **A-2•1**), 2470428 (for **A-3•1**), 2470367 (for **C-2**), 2470451 (for **C-3**), 2470420 (for **D-2**), 2470744 (for **D-3**), 2470418 (for **E-2**), and 2470368 (for **E-3**) contain the supplementary crystallographic data for this paper. These data are provided free of charge by the joint Cambridge Crystallographic Data Centre and Fachinformationszentrum Karlsruhe Access Structures service.
[35] B. Cordero, V. Gómez, A. E. Platero-Prats, M. Revés, J. Echeverría, E. Cremades, F. Barragán, S. Alvarez, *Dalton Trans.* **2008**, 2832.
[36] H. Hopöfl, *J. Organomet. Chem.* **1999**, *581*, 129.
[37] A. Konishi, R. Yasunaga, K. Chiba, M. Yasuda, *Chem. Commun.* **2016**, *52*, 3348.
[38] W. Adam, H. M. Harrer, A. Treiber, *J. Am. Chem. Soc.* **1994**, *116*, 7581.
[39] A. C. Vetter, K. Nikitin, D. G. Gilheany, *Chem. Commun.* **2018**, *54*, 5843.
[40] We performed DFT calculations for the activation of ester **4** with the $AlrBu_2$ complex **A-4**, corresponding to **A-2**, to demonstrate the importance of the high Lewis acidity of the $AlCl_2$ group in enabling the activation of less reactive carbonyl compounds (see pp. 40–42 in the Supporting Information).
[41] We confirmed that, like the other reported Al/P FLPs, complexes A also activate aldehydes and isocyanates. On the other hand, ethynylarenes were not activated, most likely because ethynylarenes cannot displace the phosphino-substituent from the aluminum center and coordinate to it, owing to the weak coordinating ability of the C–C triple bond.
[42] R. Costil, A. J. Sterling, F. Duarte, J. Clayden, *Angew. Chem. Int. Ed.* **2020**, *59*, 18670.
[43] S. Stavber, P. Kralj, M. Zupan, *Synthesis* **2002**, *11*, 1513.
[44] M. Murata, S. L. Buchwald, *Tetrahedron* **2004**, *60*, 7397.
[45] F. B. Mallory, C. K. Regan, J. M. Bohen, C. W. Mallory, A. A. Bohen, P. J. Carroll, *J. Org. Chem.* **2015**, *80*, 8.
[46] Y. Hirano, Y. Saiki, H. Taji, S. Matsukawa, Y. Yamamoto, *Heterocycles* **2008**, *76*, 1585.

Manuscript received: August 1, 2025
Revised manuscript received: September 17, 2025
Version of record online: ■■, ■■